Amplitude Distributions of Measured 21.5 GHz Indoor Channels for a Handheld Array

Nielsen, Jesper Ødum; Pedersen, Gert Frølund

Published in:
2021 15th European Conference on Antennas and Propagation (EuCAP)

DOI (link to publication from Publisher):
10.23919/EuCAP51087.2021.9411466

Publication date:
2021

Document Version
Accepted author manuscript, peer reviewed version

Amplitude Distributions of Measured 21.5 GHz Indoor Channels for a Handheld Array

Jesper Ødum Nielsen, Gert Frølund Pedersen

APMS, Dept. of Electronic Systems, Technical Faculty of IT and Design, Aalborg University, Denmark.
Email: {jni, gfp}@es.aau.dk

***Abstract*—This work investigates 21.5 GHz channel amplitude distributions for a smartphone-like mockup device used in an indoor corridor environment. Channels between an access point (AP) and the mockup were measured for different scenarios and with different users holding the mockup. In addition the mockup was measured without any user nearby in the same conditions. This allows the study of amplitude cumulative distribution functions (CDFs) both when a user is present close to the antennas of the mockup, as well as when no interaction happens. Large variations in the CDF were found both for line of sight (LOS) and non-line of sight (NLOS) scenarios. The presence of a user generally reduced the 1st percentile of the fading amplitude by 2.9 dB and 4.9 dB in median, respectively, for vertical and horizontal polarization at the AP.**

***Index Terms*—indoor radio propagation, mm-wave channels, fading statistics**

I. Introduction

The fifth generation (5G) of mobile communication networks are currently being deployed where a future new feature is the use of cm-wave and mm-wave bands [1]. Frequencies below 30 GHz are attractive due to available spectrum and expected reasonable propagation conditions [2]. The cm-wave bands are relatively new in a mobile communications context and thus these channels are not as well explored as the legacy bands below 6 GHz. At the same time it may be expected that the channels in the new bands will have different properties than sub-6 GHz channels.

For mobile communications the handheld use-case is important, in which the device and its antennas are close to the user's hand and body. In addition to possible power absorption in the human tissue, the user may also act as scatterer for signals received or transmitted form the device antennas [3]. Therefore, the user needs to be included in studies of the radio channel targeting cm-wave channels for handheld devices.

The current work investigates an indoor channel at 21.5 GHz from an AP to a smartphone-like mockup which allows to include the effects of a person holding the mockup and the dynamic effects due to user movements. Based on the measured data CDFs of channel amplitudes are estimated and analyzed.

The related work in [4] studies fading statistics for a 26 GHz point-to-point indoor static scenario. Other related previous works include [5], [6].

II. Measurements

The measurements used in this work are described in detail in [7], with only a brief description given here of the parts relevant for the current work. All measurements were carried out using the wideband correlation channel sounding system system described in [8], which was configured to operate in a 100 MHz band centered at 21.5 GHz. The system is setup in a corridor environment with a dual-polarized horn antenna pointing along the corridor, mounted at 2.05 m height near a side wall to mimic an access point.

The corridor has doors to offices along both sides; the side walls are made of plasterboard on metallic frame, and the floor and ceiling are of concrete, with an additional extra light ceiling made of plasterboard on a metallic frame, hiding various pipes, ventilation ducts, *etc.*

The mobile station (MS) is a mockup handset equipped with $R = 7$ elements, arranged as a uniform linear array (ULA) along the short side of a 110 mm $\times$ 55 mm printed circuit board (PCB). The element separation is around half the wavelength at 21.5 GHz, and the element patterns have a 5 dBi gain roughly towards the user when held as described below. Details of the array design are given in [9].

In the sounding setup, the MS is the receiver (Rx) and the dual-polarized horn is connected to the transmitter (Tx). Tx1 and Tx2 corresponds to the vertical and horizontal polarization, respectively, which are sounded simultaneously. Although the sounder supports multiple parallel Rx branches it is not desirable to have multiple coax cables connected to the mockup handset, since this will make it difficult to carry and handle naturally during the measurements. Instead a single coax is connected to a 1:8 switch located in the mockup handset (only 7 elements are connected). The set of channel impulse responses (CIRs) for all 2×7 branch combinations is denoted a channel *snapshot* below. The measurement of one snapshot took 573 μs, and the snapshot rate was 200 Hz, above the Nyquist rate for the expected changes in the channel. In the following a series of $S = 50$ snapshots will be referred to as *a measurement*.

In the setup the Tx is located about halfway in the corridor with the horn pointing towards an about 18 m long section of the corridor, ending in a closed door. Along the corridor section, 10 measurement locations are defined, L1, L2,..., L10, with L1 furthest from the Tx. About halfway there is

Presented at the *2021 15th European Conference on Antennas and Propagation (EuCAP).*
DOI: 10.23919/EuCAP51087.2021.9411466

a bend in the corridor, so that L1–L6 are in NLOS and L7–10 are in LOS of the Tx.

The handset was held by a person in so-called data mode, *i.e.*, holding the handset with both hands in front of the body at an angle of about 60° from vertical, as if using a smartphone. In order to capture snapshots in different (small-scale) locations, the handset was moved during the measurement in a circular manner, horizontally and while keeping the orientation. The radius of movement was roughly 5 cm, corresponding to about 3.5 wavelengths.

Four orientations were defined. In orientation O1 and O3, the user faces, respectively, away from and towards the Tx, while for orientation O2 and O4 the user faces either side wall.

In total more than 500 measurements were conducted, where all combinations of L1–L10 and O1–O4 are included. Many repetitions were carried out and up to 5 persons were involved, depending on location. Also so-called *free space* measurements were made, where the handset is mounted on a expanded polystyrene foam (EPS) column instead of held by a user, moving in a similar way as for the user-held case.

The measurements for each combination of location and orientation are divided in to two groups. The first group "Person" consists of all measurements with a person. Thus, this group may involve different persons and some repetitions. The second group "free space" consists of all measurements in free space, also including repetitions.

III. Data Analysis

The overall aim of the current work is to estimate and characterize the CDF of the channel amplitude with the MS at different locations and orientations. For each combination of Tx branch and Rx branch, the measured CIR can be represented as $h'(s,n) = h(s,n) + w(s,n)$, where s and n denote the discrete snapshot and delay index, respectively, and where $h(s,n)$ is the CIR sample and $w(s,n)$ is the noise component. The delay samples are given by $\tau(n) = n\Delta_\tau$ with $n \in \{0,1,\ldots,N-1\}$, $\Delta_\tau = 2.5$ ns and $N = 500$. The snapshots times are $t(s) = s\Delta_t$ where $s \in \{0,1,\ldots,S-1\}$ with $\Delta_t = 5$ ms and $S = 50$ is the number of snapshots in a measurement.

When processing the data it is essential to consider the noise that inevitable will be present in the measured CIR data. Since the noise component cannot be distinguished from the signal component in the following analysis, it is important to ensure a sufficiently high signal to noise ratio (SNR). Despite the use of automatic gain control (AGC) in the measurement system, a high SNR cannot be guaranteed in all the measurements, due to the highly dynamic channel and the wish to utilize the maximum possible measurement range. When measuring with a sufficiently large distance or number obstacles between the Tx and Rx, the path loss will be too large leading to a low SNR, but exactly where this happens is unknown in advance. Instead one has to rely on experience and testing of the acquired data.

In this work the approach is to estimate the SNR for each CIR snapshot and only include snapshots that have an SNR above a threshold of 15 dB. The instantaneous SNR for snapshot s is estimated by

$$\eta(s) = 10\log_{10}\left[\frac{P_h(s)}{P_w(s)}\right] \tag{1}$$

where the signal and noise power are estimated, respectively, as

$$\begin{aligned} P_h(s) &= \sum_{n=0}^{M-1} |h(s,n)|^2 - M\tilde{\sigma}_w^2(s) \\ P_w(s) &= M\tilde{\sigma}_w^2(s) \end{aligned} \tag{2}$$

where the signal is assumed to be contained in the first $M = 100$ samples of the CIR, corresponding to 250 ns. This was verified by visual inspection of the data. The estimated instantaneous noise density is

$$\tilde{\sigma}_w^2(s) = \frac{1}{K}\sum_{n=0}^{K-1} |h(s,N-n)|^2 \tag{3}$$

i.e., it is estimated from the last $K = 400$ samples of each CIR. Visual inspection reveals that in this part of the CIR the squared magnitude of the samples may be modeled by fluctuations around a mean value, consistent with the assumption that, due to path loss, any signal components in this delay range are much lower than the system noise.

The SNR estimation described above is done for all combinations of Tx branch index, Rx branch index and snapshot. The subsequent processing only considers data with an SNR above the threshold of 15 dB.

Narrowband channels are considered in this work, and hence a discrete Fourier transform (DFT) is applied to the measured CIRs. The sub-channels are all normalized individually over the snapshots, as

$$H_n(c,t,r,s) = H'(c,t,r,s)\left[\frac{1}{S}\sum_{s=0}^{S-1}|H'(c,t,r,s)|^2\right]^{-1/2} \tag{4}$$

where $H'(c,t,r,s)$ is the transfer function coefficient before normalization for sub-channel c, Tx index t, Rx index r, and snapshot s. Only a subset of the available sub-channels are included in the analysis, chosen based on the known sounding system frequency response. The response was configured to have a 3 dB bandwidth of about 70 MHz and defines the limits of the selected $C = 86$ sub-channels.

The subsequent analysis is based on vectors of the channel coefficients obtained by concatenating the coefficients for all combinations of sub-channels, Rx-indices, and snapshots. For a single measurement this leads to a maximum of $C \cdot R \cdot S = 86 \cdot 7 \cdot 50 = 30100$ samples, when all the corresponding SNRs are above the threshold. Several measurements may be available for a given scenario defined by the combination of location, orientation and measurement type, which are all concatenated into a single vector. The vector of complex coefficients is used to compute an empirical CDF of the amplitude,

Presented at the *2021 15th European Conference on Antennas and Propagation (EuCAP).*
DOI: 10.23919/EuCAP51087.2021.9411466

for each scenario. Since many scenarios are considered it is also useful to define a scalar metric; for this purpose the 1st percentile is used, *i.e.*, the level, in dB, below which 1% of the samples are observed.

It is noted that the sub-channels for a measurement may be correlated, depending on the channel properties, and hence the samples are not necessarily of the same value in the analysis. It should also be noted that although snapshots with low power are discarded based on the SNR, the lowest power levels in the CDF are not limited by the SNR threshold, since the power in the sub-channels are subject to fading and the SNR is determined by the total power in the wideband channel.

IV. Results

Fig. 1 shows an example of the CDF obtained when all snapshots are used, including those with low SNR, as well as the CDF obtained when only using snapshots where the instantaneous SNR is above the threshold of 15 dB. Including snapshots with low SNR increases the probability of low values, and thus closer to the CDF of a Rayleigh channel that would be the obtained if the snapshots were zero-mean Gaussian noise. Obviously, the Rayleigh channel may be the correct result, even in the noise-less case, so the SNR is needed for quality evaluation.

An impression of where the censoring of snapshots with low SNR is most important can be obtained from Table I. For each location L1, ..., L10, there are 16 combinations of orientation, Tx, and measurement type (free space or person). The table lists for each location the min/max of the percentage of snapshots that are included in the processing, where the min/max is evaluated among the combinations for each location. Similarly, min/max of the number of snapshots are given. It is noted that the low snapshot SNR is mainly a problem for L2/L3 which are furthest away from the Tx. For the remaining locations more than 90 % of the snapshots are included in the estimation. It should be noted that in Table I for L2, the combinations O1/FreeSpace/Tx2, O1/Person/Tx2, and O4/FreeSpace/Tx1 are not included in the statistics since measurements are either missing or too low quality, and hence no CDF curves were produced at all.

The results discussed henceforth are based on snapshots with instantaneous SNRs above the 15 dB threshold.

Fig. 2 shows an overview of the 1st percentiles obtained for the different scenarios. A first observation is that all values are above -20 dB and therefore the channels are in all cases less likely to have deep fades than a Rayleigh channel.

For free space scenarios the percentiles vary highly among the locations and orientations with values from about -19.5 dB to -2 dB. In some cases the orientation alone can cause dramatic changes in the CDF, for example at L9 for Tx1. The CDF for these cases are shown in Fig. 3. One may conjecture that this is because L9 is in LOS of the AP and hence the orientation of the directive antennas has a major impact. However, the orientation also has a large impact, *e.g.*, at L3 and L6, both of which are in NLOS. A possible explanation might be that even in NLOS there will be some main signal directions due to the guiding effect of the corridor.

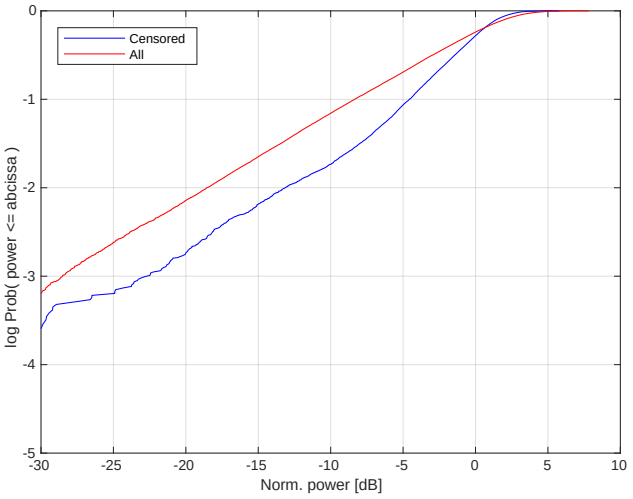

Fig. 1. Estimated CDF curves with and without censoring of snapshots with low SNR for the scenario L3, O1, Tx2, with person.

TABLE I
The number of samples included in the CDF estimation, shown as minimum and maximum among all combinations of orientations, Tx, and measurement type. Note exceptions mentioned in text.

Location	Min. %	Min. no.	Max. %	Max. no.
L2	22	$1.3 \cdot 10^4$	89	$1.1 \cdot 10^5$
L3	35	$1.6 \cdot 10^4$	100	$1.5 \cdot 10^5$
L4	93	$2.8 \cdot 10^4$	100	$1.5 \cdot 10^5$
L5	91	$2.7 \cdot 10^5$	100	$8.4 \cdot 10^5$
L6	99	$3.0 \cdot 10^4$	100	$1.5 \cdot 10^5$
L7	99	$3.0 \cdot 10^5$	100	$8.7 \cdot 10^5$
L8	97	$3.0 \cdot 10^4$	100	$1.5 \cdot 10^5$
L9	100	$3.0 \cdot 10^4$	100	$1.5 \cdot 10^5$
L10	99	$3.0 \cdot 10^4$	100	$1.2 \cdot 10^5$

For the scenarios including a person, the variation among the orientations are generally smaller than for free space, and the highest are lower than they are for free space. A possible explanation for this is that the main direction of the elements are towards the person holding the handset, who will thus either block the direction towards the AP or act as a scatterer. Examples of CDF curves for cases with a person are shown in Fig. 4.

With the purpose of showing the overall impact of the presence of a user has, all the data is sorted into groups defined by the four combinations of Tx index and measurement type, so that each group contain 1st percentiles for all combinations of locations and orientations. A boxplot of the 1st percentiles for the groups is shown in Fig. 5. The upper and lower limit of each box is defined by the 1st and 3rd quartiles, respectively, and the vertical lines represent the extend of the data, not counting outliers shown as red points. The median is shown as a red line in the box.

From Fig. 5 it is clear that the presence of a person holding the handset in general tend to lower the 1st percentile, with

Presented at the *2021 15th European Conference on Antennas and Propagation (EuCAP).*
DOI: 10.23919/EuCAP51087.2021.9411466

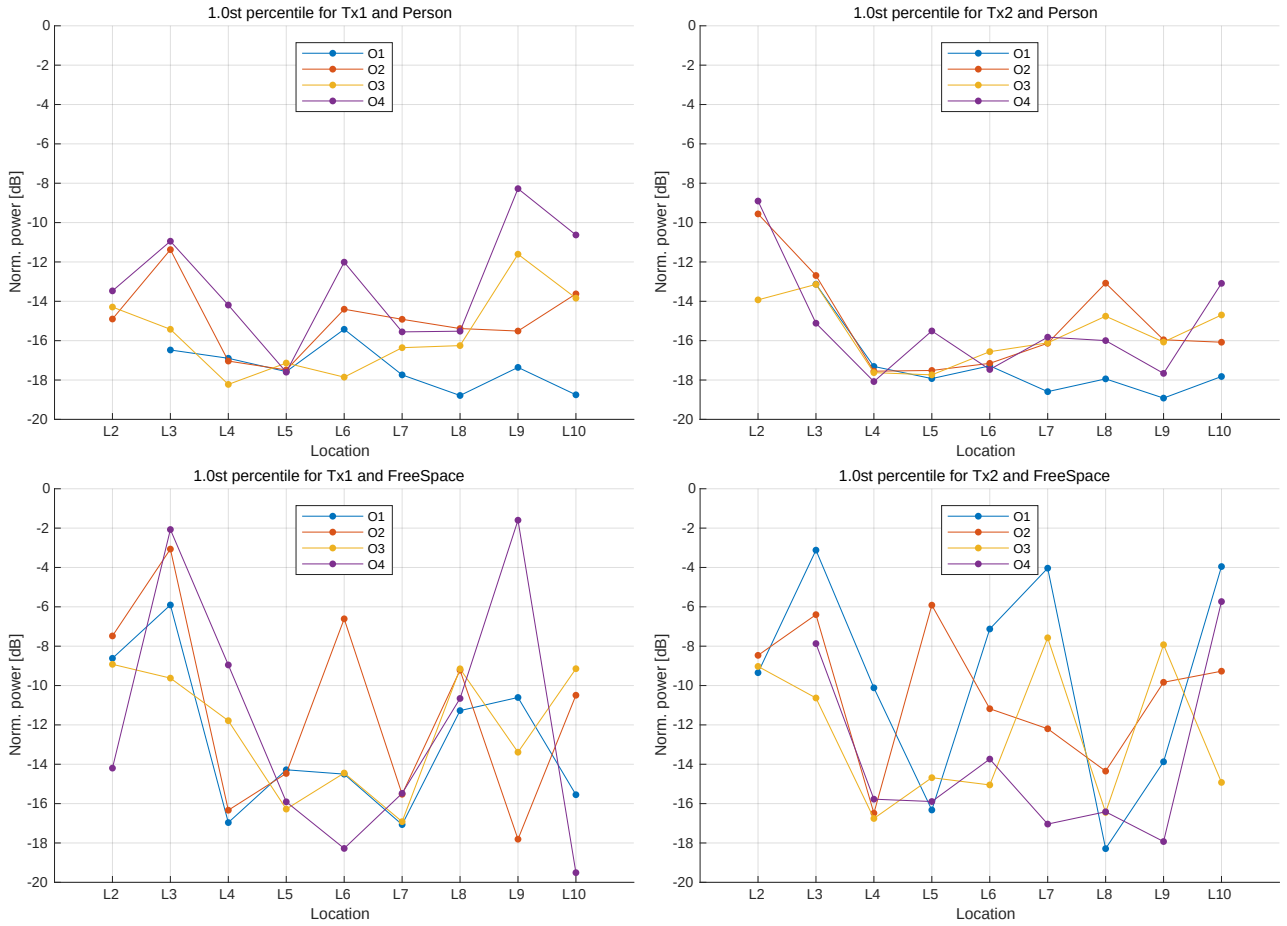

Fig. 2. 1st percentiles for all combinations of location, orientation, measurement type and Tx. Note only points represent data, lines are only for visual aid.

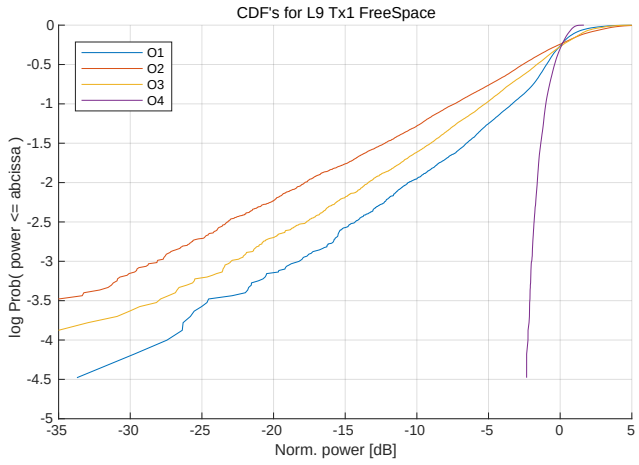

Fig. 3. Empirical CDFs for L9, Tx1 in free space and for the four orientations.

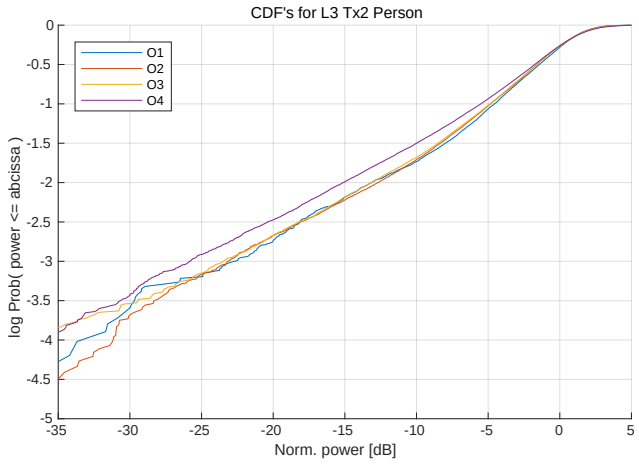

Fig. 4. Empirical CDFs for L3, Tx2 with a person and for the four orientations.

a change in median of 2.9 dB and 4.9 dB, for Tx1 and Tx2, respectively. Also the variation among the locations and orientations are reduced, as indicated by 1st to 3rd quartile interval, which is reduced from 6.7 dB to 3.4 dB, and 8.0 dB to 2.9 dB, respectively for Tx1 and Tx2.

It is noted that the changes in both median and quartile interval are larger for the horizontally polarized Tx2, than for the vertically polarized Tx1.

Presented at the *2021 15th European Conference on Antennas and Propagation (EuCAP).*
DOI: 10.23919/EuCAP51087.2021.9411466

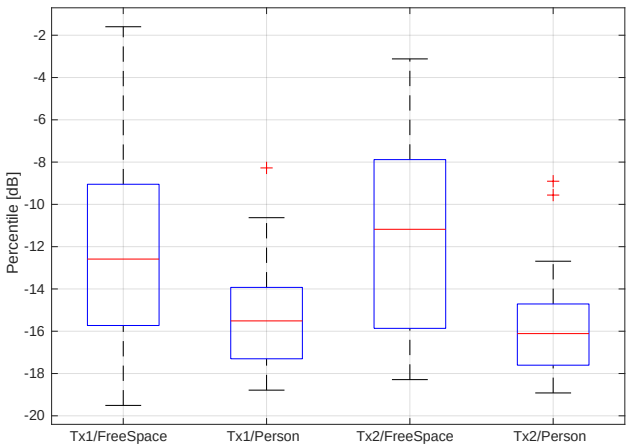

Fig. 5. Boxplot of 1st percentiles with Tx and measurement type as parameters.

V. Conclusions

This work investigates amplitude distributions of a channel between an AP and a handheld device operating in the 21.5 GHz band in an indoor corridor environment. The work is based on wideband measurements in scenarios defined by combinations of 9 locations, 4 orientations, 2 AP polarizations and with or without a user holding the mockup handset.

An important aspect when estimating a CDF from measured data is the SNR, since insufficient SNR may cause the noise to mask the properties of channel gain. In the analysis the SNRs of the individual snapshots are estimated to ensure a minimum of 15 dB SNR.

A considerable variation in the CDFs were found and to ease comparison, the 1st percentile has been used as a simple scalar metric which is free from model assumptions. All estimated 1st percentiles are above -20 dB, indicating channels that have less frequent fades than a Rayleigh channel. The percentiles were all between about -19.5 dB and -2 dB, with high values found for both LOS and NLOS scenarios, contrary to what might be expected.

The presence of a user holding the handset, as opposed to being in free space, generally reduces the 1st percentile with changes in median values of 2.9 dB and 4.9 dB for the case of using, respectively, vertical and horizontal polarization on the AP. The presence of a user also generally reduces the variation in the observed 1st percentiles.

Acknowledgment

This work was supported by the Danish National Advanced Technology Foundation project “Virtuoso.”

References

[1] Q. C. Li, H. Niu, A. T. Papathanassiou, and G. Wu, “5G network capacity: Key elements and technologies,” *IEEE Vehicular Technology Magazine*, vol. 9, no. 1, pp. 71–78, 2014.

[2] M. Samimi, K. Wang, Y. Azar, G. N. Wong, R. Mayzus, H. Zhao, J. K. Schulz, S. Sun, F. Gutierrez, and T. S. Rappaport, “28 GHz angle of arrival and angle of departure analysis for outdoor cellular communications using steerable beam antennas in new york city,” in *Vehicular Technology Conference (VTC Spring), 2013 IEEE 77th*, June 2013, pp. 1–6.

[3] I. Syrytsin, S. Zhang, G. F. Pedersen, K. Zhao, T. Bolin, and Z. Ying, “Statistical investigation of the user effects on mobile terminal antennas for 5G applications,” *IEEE Trans. Antennas Propag.*, vol. 65, no. 12, pp. 6596–6605, 2017.

[4] K. Saito, T. Imai, and Y. Okumura, “Fading characteristics in the 26GHz band indoor quasi-static environment,” in *2014 IEEE International Workshop on Electromagnetics (iWEM)*, 2014, pp. 135–136.

[5] N. Iqbal, C. Schneider, J. Luo, D. Dupleich, R. Müller, S. Haefner, and R. S. Thomä, “On the stochastic and deterministic behavior of mmwave channels,” in *11th European Conference on Antennas and Propagation (EUCAP)*, 2017, pp. 1813–1817.

[6] M. K. Samimi, G. R. MacCartney, S. Sun, and T. S. Rappaport, “28 GHz millimeter-wave ultrawideband small-scale fading models in wireless channels,” in *83rd Vehicular Technology Conference (VTC Spring)*, May 2016, pp. 1–6.

[7] J. Hejselbæk, J. Ø. Nielsen, W. Fan, and G. F. Pedersen, “Measured 21.5 GHz indoor channels with user-held handset antenna array,” *IEEE Trans. Antennas Propag.*, vol. 65, no. 12, pp. 6574–6583, Dec 2017.

[8] J. Ø. Nielsen, W. Fan, P. C. F. Eggers, and G. F. Pedersen, “A channel sounder for massive MIMO and MmWave channels,” *IEEE Commun. Mag.*, vol. 56, no. 12, pp. 67–73, December 2018.

[9] N. Ojaroudiparchin, M. Shen, S. Zhang, and G. Pedersen, “A switchable 3d-coverage phased array antenna package for 5g mobile terminals,” *IEEE Antennas Wireless Propag. Lett.*, vol. 15, pp. 1747 – 1750, Feb. 2016.

Presented at the *2021 15th European Conference on Antennas and Propagation (EuCAP).*
DOI: 10.23919/EuCAP51087.2021.9411466